

# Comprehensive Study of Convex-Louver and Wavy Fin-and-Tube Heat Exchangers

Chi-Chuan Wang\*

Industrial Technology Research Institute, Chutung, Hsinchu, Taiwan 310, Republic of China  
and

Yu-Min Tsai† and Ding-Chong Lu‡

National Chiao Tung University, Hsinchu, Taiwan 300, Republic of China

A comprehensive study to investigate the heat transfer and friction characteristics of convex-louver and wavy fin-and-tube heat exchangers was carried out in this study. A total of 14 samples of heat exchangers, including seven convex-louver and seven wavy fin samples having identical waffle heights, were tested and compared in the present investigation. The effects of the number of tube row and fin pitch on the thermal-hydraulic characteristics were also reported. Results were presented as plots of Fanning friction factor  $f$  and the Colburn  $j$  factor against a Reynolds number based on a tube collar diameter in the range of  $3 \times 10^2$  to  $8 \times 10^3$ .

## Nomenclature

$A$	= area, $\text{m}^2$
$A_t$	= external tube surface area, $\text{m}^2$
$A_o$	= total surface area, $\text{m}^2$
$b$	= spacing between the two corrugated channel walls, mm
$C$	= heat-capacity rate, $\text{W/K}$
$c_p$	= specific heat at constant pressure, $\text{J/(kg K)}$
$D_c$	= fin collar o.d., m
$D_i$	= inside tube diameter, m
$F_p$	= fin pitch, mm
$f$	= Fanning friction factor, dimensionless
$G_c$	= mass flux of the air based on the minimum flow area, $\text{kg/(m}^2 \text{ s)}$
$h$	= heat transfer coefficient, $\text{W/(m}^2 \text{ K)}$
$j$	= Colburn factor, $Nu/RePr^{1/3}$ , dimensionless
$K_c$	= abrupt contraction pressure-loss coefficient
$K_e$	= abrupt expansion pressure-loss coefficient
$k$	= fluid thermal conductivity, $\text{W/(m K)}$
$L_p$	= louver pitch, mm
$\dot{m}$	= mass flow rate, $\text{kg/s}$
$N$	= number of longitudinal tube rows, dimensionless
$NTU$	= number of transfer unit, $U \cdot A/C_{\min}$ , dimensionless
$P_f$	= fin pitch, mm
$P_l$	= longitudinal tube pitch, mm
$Pr$	= Prandtl number, dimensionless
$P_t$	= transverse tube pitch, mm
$\dot{Q}$	= heat transfer rate, $\text{W}$
$\dot{Q}_{\max}$	= maximum possible heat transfer rate, $C_{\min}(T_{\text{water,in}} - T_{\text{air,in}})$ , $\text{W}$
$Re_{D_c}$	= Reynolds number based on tube o.d., including collar, dimensionless, $\rho V D_c / \mu$
$Re_L$	= Reynolds number based on the louver pitch, $L_p$ , $\rho V L_p / \mu$ , dimensionless

$R_{eq}$	= equivalent radius for circular fin, mm
$r$	= radius of the tube diameter, including collar fin thickness, mm
$T$	= temperature, $^{\circ}\text{C}$
$t$	= fin thickness, mm
$U$	= overall heat transfer coefficient, $\text{W/(m}^2 \text{ K)}$
$V$	= velocity, $\text{m/s}$
$X_L$	= geometric parameter $\sqrt{(P_t/2)^2 + P_l^2}/2$ , mm
$X_M$	= $P_t/2$ , geometric parameter, mm
$\Delta P$	= pressure drop, $\text{Pa}$
$\delta$	= thickness of tube wall, mm
$\varepsilon$	= heat exchanger effectiveness, $\dot{Q}_{av}/\dot{Q}_{\max}$ , dimensionless
$\eta$	= fin efficiency, dimensionless
$\eta_o$	= surface effectiveness, dimensionless
$\theta$	= ramp angle, $\text{deg}$
$\mu$	= dynamic viscosity of fluid, $\text{Pa} \cdot \text{s}$
$\rho$	= mass density of fluid, $\text{kg/m}^3$
$\sigma$	= contraction ratio of cross-sectional area, dimensionless

## Subscripts

air	= air side
av	= average value of tube side and air side
$b$	= base surface
$f$	= fin surface
$i$	= tube side
in	= inlet
$m$	= mean value of the inlet and outlet conditions
max	= maximum value
min	= minimum value
std	= arbitrarily selected temperature and pressure conditions
$w$	= wall of the tube
water	= water side
0	= total surface
1	= air-side inlet
2	= air-side outlet

## Introduction

THE heat transfer performance of an air-cooled heat exchanger is highly dependent on the pattern of fins because the dominant thermal resistance is generally on the air side. Figure 1 shows the common plate fin-and-tube heat exchangers, including plain, wavy, louver, and convex-louver. For

Received April 16, 1997; revision received Dec. 9, 1997; accepted for publication Dec. 12, 1997. Copyright © 1998 by the American Institute of Aeronautics and Astronautics, Inc. All rights reserved.

\*Senior Researcher, Energy and Resources Institute, D500, Building 64, 195-6 Section 4, Chung Hsing Road. E-mail: f781058@erlib.eri.itri.org.tw.

†Graduate Assistant, Department of Mechanical Engineering.

‡Professor, Department of Mechanical Engineering.

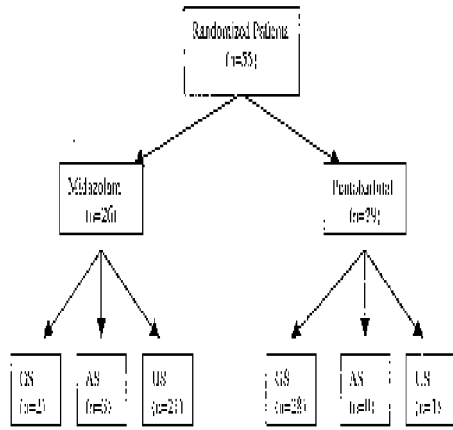


**Fig. 1** Schematic of various fin patterns of plate fin-and-tube heat exchangers.

space-limited application, the use of enhanced fins is particularly helpful because considerable size reduction can be achieved. Therefore, the enhanced fin patterns such as louver fin and convex-louver are popular in residential and commercial utilization.

The convex-louver fin is a combination of the wavy and louver fin geometries. There are many extensive experimental data related to the wavy fin geometry<sup>1-3</sup> and louver fin geometry.<sup>4-6</sup> However, only relatively few experimental data were associated with the convex-louver fin patterns. The only published experimental data associated with convex-louver geometry were reported by Hadata et al.<sup>7</sup> and Wang et al.<sup>8</sup> Hadata et al. indicated that the heat transfer coefficient of the convex-louver fin is 2.8 times higher than that of the plain fin at the same air velocity with a pressure drop approximately 3.3 times higher than that of the plain fin geometry. Wang et al.<sup>8</sup> showed that the Colburn  $j$  factors for convex-louver fin were 99–183% higher than those of plain fin. This is a 21–48% increase as compared to wavy fin geometry and is comparable to the louver fin pattern. The tubes used by previous investigators in their fin-and-tube heat exchangers were either 10 or 15.88 mm. Recently, the use of even smaller tubes, e.g., 7.94 mm, in residential applications are gaining popularity. This is because higher heat transfer coefficients, lower pressure drops, and less refrigerant charge in the system can be achieved by using smaller tubes and result in much more compact fin-and-tube heat exchanger design. The major objective of this study is to provide systematically updated information on the air-side performance of previous efforts<sup>3,8</sup> with a considerable enlargement of scope. Furthermore, in-depth interpretation of the test results are made to clarify several unusual characteristics of the convex-louver and wavy fin patterns.

### Experimental Apparatus

A total of 14 heat exchangers were tested in the present study, including seven convex-louver fins and seven wavy fins. Detailed dimensions of convex-louver and wavy fin patterns are illustrated in Fig. 2. Geometric parameters of the present test samples are tabulated in Table 1. All tests were conducted in an open wind tunnel as shown in Fig. 3. The ambient airflow is forced across the test section by means of a 5.6-kW centrifugal fan with an inverter. To avoid and minimize the effect of flow maldistribution in the experiments, an air straightener-equalizer and a mixer were provided. The inlet and exit temperatures across the sample coil were measured by two T-type thermocouple meshes. The inlet measuring mesh consists of 12 thermocouples, whereas the outlet mesh contains 36 thermocouples. The sensor locations inside the rectangular duct were established following the American Society of Heating, Refrigerating and Air-Conditioning Engineers (ASHRAE) recommendation.<sup>9</sup> These data signals were individually recorded

and then averaged. During the isothermal test, the variance of these thermocouples was within  $\pm 0.2^\circ\text{C}$ . All of the thermocouples were precalibrated by a quartz thermometer with  $0.01^\circ\text{C}$  precision.

The pressure drop of the test coil is detected by a precision differential pressure transducer, reading to 0.1 Pa. The airflow-measuring station is a multiple-nozzle code tester based on the ASHRAE 41.2 standard.<sup>10</sup> The working medium in the tube side was hot water. The inlet water temperature was controlled by a thermostat reservoir having an adjustable capacity up to 60 kW. Both the inlet and outlet temperatures were measured by two precalibrated resistance temperature devices (RTDs, Pt-100 $\Omega$ ). Their accuracy was within  $0.05^\circ\text{C}$ . The water volumetric flow rate was detected by a magnetic flow meter with 0.002 L/s resolution.

All of the data signals were collected and converted by a data-acquisition system (a hybrid recorder). The data-acquisition system then transmitted the converted signals through a general purpose interface bus to the host computer for further operation. During the experiments the water inlet temperature was held constant at  $65.0 \pm 0.3^\circ\text{C}$ , and the tube-side Reynolds number was approximately  $3.5 \times 10^4$ . Frontal velocities ranged from 0.3 to 6.5 m/s. During the test, the energy imbalance between the air side and the tube side was within 3%.

### Data Reduction

To obtain the heat transfer and pressure-loss characteristics of the test coil from the experimental data, the  $\varepsilon$ - $NTU$  method is applied to determine the  $UA$  product in the analysis. The total heat transfer rate used in the calculation is the mathematical average of the air-side and the water-side heat transfer rates, namely,

$$\dot{Q}_{\text{air}} = \dot{m}_{\text{air}} c_{p,\text{air}} \Delta T_{\text{air}} \quad (1)$$

$$\dot{Q}_{\text{water}} = \dot{m}_{\text{water}} c_{p,\text{water}} \Delta T_{\text{water}} \quad (2)$$

$$\dot{Q}_{\text{av}} = (\dot{Q}_{\text{water}} + \dot{Q}_{\text{air}})/2 \quad (3)$$

In the  $\varepsilon$ - $NTU$  method, the number of heat transfer units ( $NTU$ ) is defined as

$$NTU \equiv UA/C_{\min} \quad (4)$$

The maximum heat capacity  $C_{\max}$  is always on the tube side in the present study. The  $UA$  product was calculated using the  $\varepsilon$ - $NTU$  method for unmixed-unmixed crossflow. Correspondingly, the appropriate  $\varepsilon$ - $NTU$  relationship<sup>11</sup> is

$$\varepsilon = 1 - \exp\{NTU^{0.22}/C^* \cdot [\exp(-C^* \cdot NTU^{0.78}) - 1]\} \quad (5)$$

where

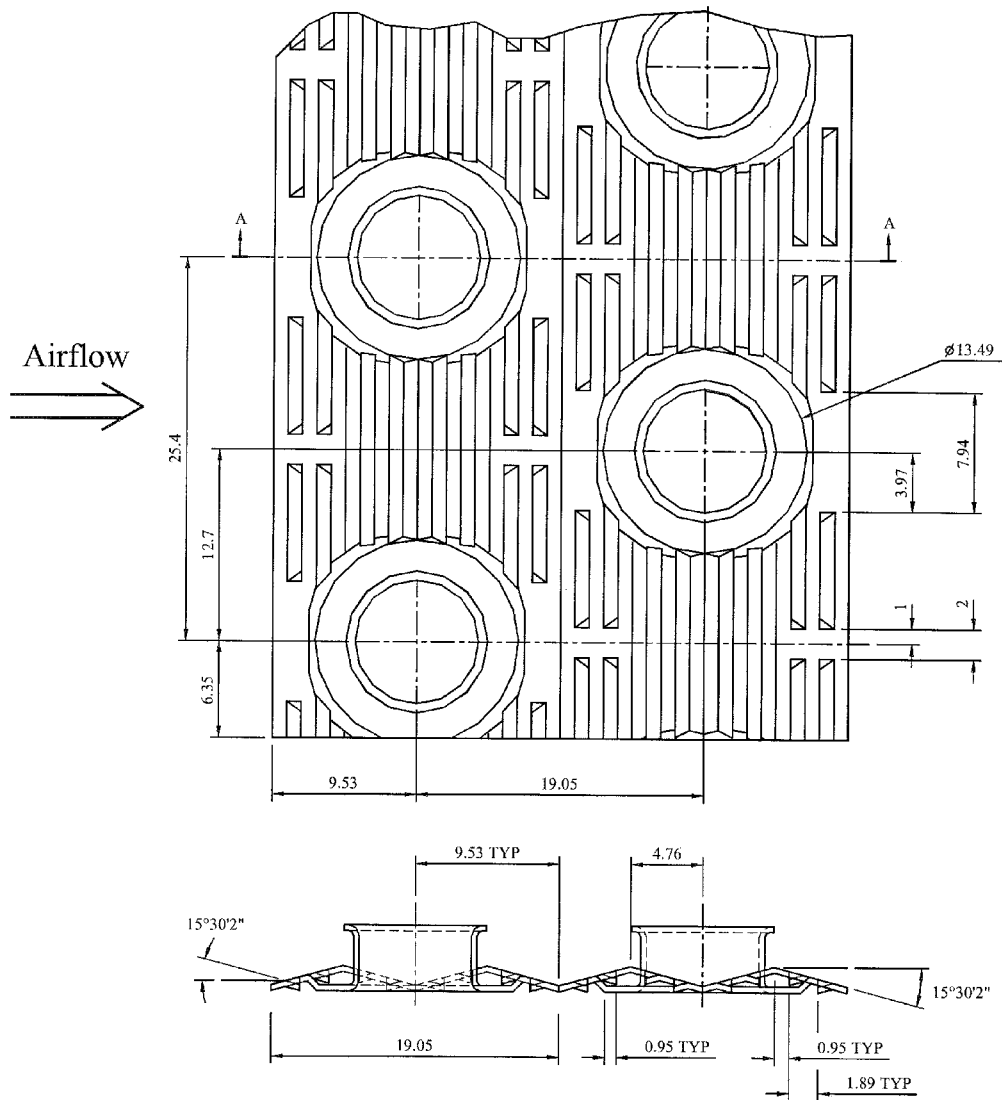
$$C^* \equiv \frac{C_{\min}}{C_{\max}} = \frac{\dot{m}_{\text{air}} c_{p,\text{air}}}{\dot{m}_{\text{water}} c_{p,\text{water}}} \quad (6)$$

$$\varepsilon \equiv \frac{\dot{Q}_{\text{av}}}{\dot{Q}_{\max}} = \frac{\dot{Q}_{\text{av}}}{\dot{m}_{\text{water}} c_{p,\text{water}} (T_{\text{in,water}} - T_{\text{in,air}})} \quad (7)$$

The overall heat transfer resistance is defined from the following relationship:

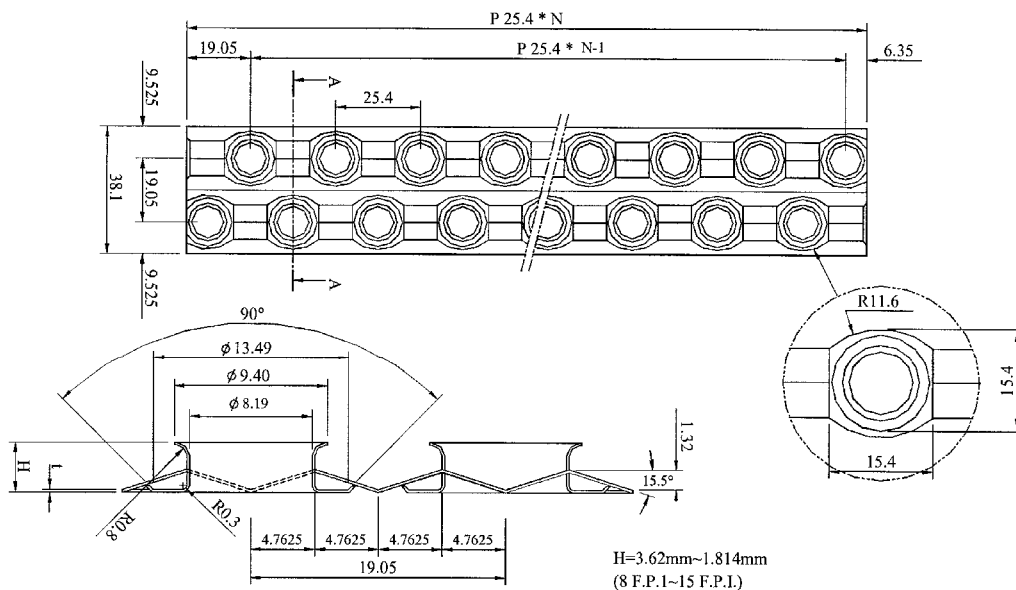
$$\frac{1}{UA} = \frac{1}{\eta_0 h_0 A_0} + \frac{\delta_w}{k_w A_w} + \frac{1}{h_i A_i} \quad (8)$$

Note that the surface area used in the present investigation is the actual surface area of the wavy fin pattern. The tube-side



a)

## SECTION - AA



b)

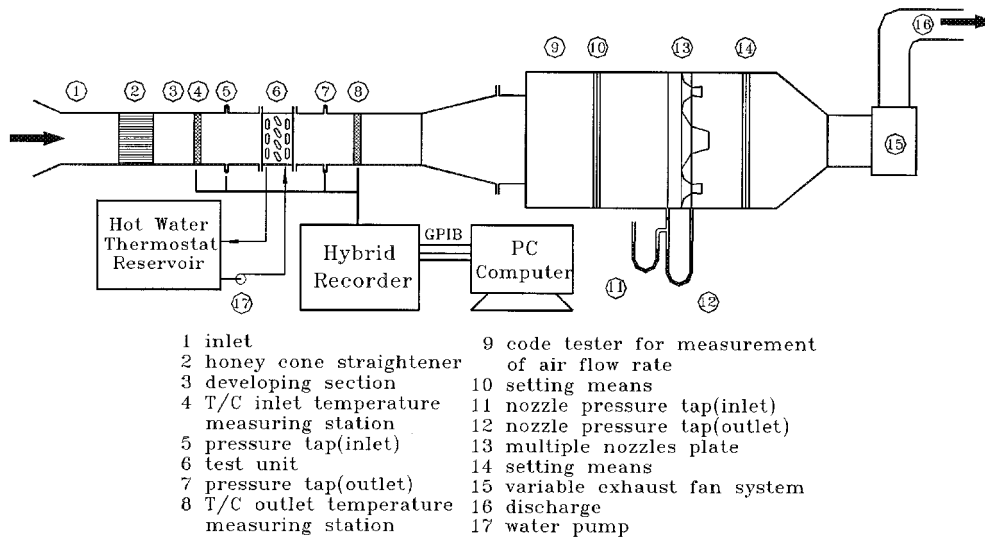
## SECTION A-A 4/1

Fig. 2 a) Convex-louver fin and b) wavy fin geometries tested in the present investigation (units in millimeters).

**Table 1** Geometric dimensions of the sample heat exchangers<sup>a</sup>

No.	Fin pattern	Fin pitch, mm	$D_o^b$ , mm	$P_p$ , mm	$P_b$ , mm	Number of tube row
1	Convex-louver	2.54	8.54	25.4	19.05	1
2	Wavy	2.54	8.54	25.4	19.05	1
3	Convex-louver	1.21	8.54	25.4	19.05	1
4	Wavy	1.21	8.54	25.4	19.05	1
5	Convex-louver	2.54	8.54	25.4	19.05	2
6	Wavy	2.54	8.54	25.4	19.05	2
7	Convex-louver	1.69	8.54	25.4	19.05	2
8	Wavy	1.69	8.54	25.4	19.05	2
9	Convex-louver	1.21	8.54	25.4	19.05	2
10	Wavy	1.21	8.54	25.4	19.05	2
11	Convex-louver	2.54	8.54	25.4	19.05	4
12	Wavy	2.54	8.54	25.4	19.05	4
13	Convex-louver	1.21	8.54	25.4	19.05	4
14	Wavy	1.21	8.54	25.4	19.05	4

<sup>a</sup>Fin thickness of the test samples are all 0.115 mm. <sup>b</sup>Tube diameter before expansion is 7.94 mm.

**Fig. 3** Schematic of the test setup.

heat transfer coefficient  $h_i$  is evaluated from the Gnielinski<sup>12</sup> semiempirical correlation:

$$h_i = \left( \frac{k}{D} \right)_i \frac{(Re_i - 1000)Pr(f_i/2)}{1 + 12.7\sqrt{f_i/2}(Pr^{2/3} - 1)} \quad (9)$$

where

$$f_i = [1.58 \ln(Re_i) - 3.28]^{-2} \quad (10)$$

where  $Re_i = \rho V D_i / \mu$ . The surface efficiency  $\eta_o$  is defined as the actual heat transfer for the fin and base divided by the heat transfer for the fin and base when the fin is at the same base temperature  $T_b$ . This term may be written in terms of the fin efficiency  $\eta$ , fin surface area  $A_f$ , and total surface area  $A_o$

$$\eta_o = 1 - (A_f/A_o)(1 - \eta) \quad (11)$$

where  $A_o = A_f + A_b$ , and  $A_f$  and  $A_b$  are the areas of the fin and base, respectively. The  $\eta$  is calculated by the approximation method described by Schmidt<sup>13</sup>:

$$\eta = \frac{\tanh(mr\phi)}{mr\phi} \quad (12)$$

where

$$m = \sqrt{2h_o/k_f t} \quad (13)$$

$$\phi = [(R_{eq}/r) - 1][1 + 0.35 \ln(R_{eq}/r)] \quad (14)$$

$$\frac{R_{eq}}{r} = 1.27 \frac{X_M}{r} \left( \frac{X_L}{X_M} - 0.3 \right)^{1/2} \quad (15)$$

With Eqs. (12–15), an iterative procedure is needed to obtain the air-side heat transfer coefficient  $h_o$  and the surface efficiency  $\eta_o$ . The air-side heat transfer characteristics are presented in terms of the Colburn  $j$  factor:

$$j = \frac{h_o}{\rho V_{\max} C_p} Pr^{2/3} \quad (16)$$

All of the fluid properties are evaluated at the average values of the inlet and outlet temperatures under the steady-state condition. Contact resistances provided by the manufacturer are always less than 3.2% of the total resistance for the test range and are neglected in the final reduction.

The core friction of the heat exchanger is calculated from the pressure-drop equation proposed by Kays and London,<sup>14</sup> including the entrance and exit pressure-loss coefficients  $K_c$

and  $K_e$ . The relation for the nondimensional  $f$  in terms of pressure drop is shown next:

$$f = \frac{A_c}{A_o} \frac{\rho_m}{\rho_1} \left[ \frac{2\rho_1 \Delta P}{G_c^2} - (K_c + 1 - \sigma^2) - 2 \left( \frac{\rho_1}{\rho_2} - 1 \right) + (1 - \sigma^2 - K_e) \frac{\rho_1}{\rho_2} \right] \quad (17)$$


where  $A_o$  and  $A_c$  stand for the total surface area and the flow cross-sectional area, respectively. The term  $\sigma$  is the ratio of the minimum flow area to the frontal area. Core entrance and exit losses were subtracted.  $K_c$  and  $K_e$  (the abrupt contraction and expansion coefficients) were evaluated from Fig. 14-26 of McQuiston and Parker.<sup>11</sup> Uncertainties in the reported experimental values of the  $j$  and  $f$  factors were estimated by the method suggested by Moffat.<sup>15</sup> The uncertainties ranged from 3.9 to 17.2% for the  $j$  factor and from 4.7 to 25.2% for the  $f$  factor. The highest uncertainties were associated with the lowest Reynolds number.

### Results and Discussion

The experimentally determined heat transfer coefficients for the corresponding convex-louver and wavy fin having a 1-row configuration are shown in Fig. 4. As expected, the pressure drops for convex-louver fin patterns are much higher than those of the wavy fin pattern. For a very low frontal velocity ( $V_{fr} = 0.3$  m/s), where the effect of forced convection is very small, the heat transfer performances of the wavy fin and convex-louver are approximately the same regardless of the fin pitch. Further increasing frontal velocities for the wavy fin configuration results in a significant increase of heat transfer coefficient. As shown in Fig. 4 the increase of heat transfer coefficients for  $F_p = 1.21$  mm is significantly higher than those of  $F_p = 2.54$  mm. The results are consistent with the flow pattern observations of previous investigators.<sup>16-18</sup> Figure 5 illustrates the effect of fin spacing on flow pattern observed by Molki and Yuen.<sup>18</sup> In the case of smallest fin spacing the recirculation zone is relatively small. For the other two cases, where the fin spacing is increasing, the separation zone consistently expanded. Consequently, lower heat transfer coefficients are encountered by increasing fin spacing. However, with a further increase of frontal velocities ( $V_{fr} > 5$  m/s), the effect of fin pitch diminishes. This is because the vortex shedding caused by the tube starts to take effect.

For the convex-louver fin configuration, the corresponding heat transfer coefficients are approximately 21% higher than those of wavy fins for  $F_p = 2.54$  mm, and they give only 15% higher pressure drops. Decreasing the fin pitch by half to  $F_p = 1.21$  mm, the corresponding heat transfer coefficients for the convex-louver fin are 28 and 41% higher for  $V_{fr} = 1.5$  and 4.5 m/s, respectively, whereas the pressure drops are 60 and 72% higher. However, it is interesting to see that the heat transfer enhancement ratios for the convex-louver fin, evaluated as  $h_{CLF}/h_{wavy}$ , decrease with a decrease of fin pitch. For  $F_p = 1.21$  mm and  $V_{fr} < 1.0$  m/s, the heat transfer performance of the wavy and convex-louver fin were approximately the same, but the convex-louver fin shows a 30–40% higher pressure drop. This suggests that the convex-louver may not be so effective in the low-velocity range.

For a detailed comparison between the convex-louver and wavy fin configurations, the VG-1 performance criteria were adopted. A detailed description of this method can be found in Webb.<sup>19</sup> The VG-1 criteria seek the possibility of reducing the surface area for using the enhanced fin surface having a fixed pumping power, heat duty, and temperature difference. Figure 6 shows the performance benefits of using the convex-louver fin surface relative to the wavy fin surface having a 1-row configuration. As seen, for  $F_p = 1.21$  mm and  $Re_{Dc,wavy} < 1 \times 10^3$ , area reduction is not attainable by using the convex-louver fin. A maximum reduction of 18% is seen for the  $F_p = 2.54$



**SAEM**

## CALL FOR ABSTRACTS

**2001 Annual Meeting**  
May 6-9 — Atlanta

The Program Committee is accepting abstracts for review for oral and poster presentation at the 2001 SAEM Annual Meeting. Authors are invited to submit original research in all aspects of Emergency Medicine including, but not limited to: abdominal/gastrointestinal/genitourinary pathology, administrative/health care policy, airway/anesthesia/analgesia, CPR, cardiovascular (non-CPR), clinical decision guidelines, computer technologies, diagnostic technologies/radiology, disease/injury prevention, education/professional development, EMS/out-of-hospital, ethics, geriatrics, infectious disease, Innovations in EMI Education exhibit, ischemia/reperfusion, neurology, obstetrics/gynecology, pediatrics, psychiatry/social issues, research design/methodology/statistics, respiratory/ENT disorders, shock/critical care, toxicology/environmental injury, trauma, and wounds/burns/orthopedics.

The deadline for submission of abstracts is January 9, 2001 at 3:00 pm Eastern Time and will be strictly enforced. Only electronic submissions via the SAEM online abstract submission form will be accepted. The abstract submission form and instructions will be available on the SAEM web site at [www.saem.org](http://www.saem.org) by November 1, 2000. For further information or questions, contact SAEM at [saem@saem.org](mailto:saem@saem.org) or 517-485-5484 or via fax at 517-485-0601.

Only reports of original research may be submitted. The data must not have been published in manuscript or abstract form or presented at a national medical scientific meeting prior to the 2001 SAEM Annual Meeting. Original abstracts presented at other national meetings within 30 days prior to the 2001 Annual Meeting will be considered.

Abstracts accepted for presentation will be published in the May issue of *Academic Emergency Medicine*, the official journal of the Society for Academic Emergency Medicine. SAEM strongly encourages authors to submit their manuscripts to AEM. AEM will notify authors of a decision regarding publication within 60 days of receipt of a manuscript.

Society for Academic Emergency Medicine • 901 North Washington Avenue • Lansing, MI 48906

Fig. 4 Heat transfer coefficients and pressure drops for the convex-louver/wavy fin having a 1-row configuration.

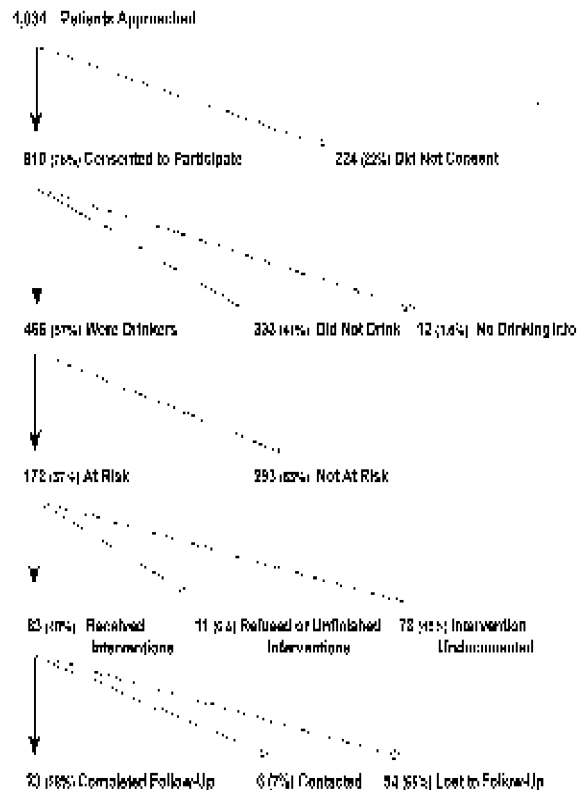


Fig. 5 Patterns of fluid flow in corrugated channel.

mm, and the maximum area reduction occurs near  $Re_{Dc} = 2.1 \times 10^3$  (based on  $Re_{Dc,wavy}$ ). The curve shows that the air-side enhancement is less beneficial as the fin pitch decreases.

Comparing the present convex-louver and wavy fin patterns, it appears that the wavy fin shows less dependence of fin pitch. This phenomenon is particularly evident for multiple-row coils as shown by Fig. 7. As seen, the fin pitch shows a negligible effect on the heat transfer performances. The present results agree with those reported by Wang et al.<sup>3</sup> Note that the waffle

height of the test coils by Wang et al. was 1.5 mm compared to the present 1.32 mm. The small dependence of fin pitch for a multiple-row coil having a plain fin pattern was also reported by Rich<sup>20</sup> and Wang et al.<sup>21</sup> An explanation for the independence of fin pitch for the wavy fin patterns may be because of the disturbance caused by the tubes. Conversely to the test results of the plain and wavy fins, the convex-louver fin shows a mild dependence of fin pitch as indicated by Fig. 7. This phenomenon is especially pronounced for large fin pitch ( $F_p = 2.54$  mm). As seen in Fig. 7, the heat transfer performances for  $F_p = 2.54$  mm are approximately 20% lower than those of  $F_p = 1.21$  and 1.69 mm. The test results for the present convex-louver fin are consistent with previous findings by Wang et al.<sup>8</sup> (10.3 mm tube diameter); however, they did not give any explanation about this phenomenon. The differences in the effect of fin pitch between the convex-louver fin and the wavy fin patterns can be explained from the flow visualization experiments of convex-strip conducted by Pauley and Hodgson.<sup>22</sup>

For a particular fin pitch and waffle height of a convex-louver strip, Pauley and Hodgson reported that the mixing angle usually increased with an increase in Reynolds number. Note that mixing angle is defined as the inclined angle formed by the dye, as measured from the louver of first contact. Pauley

and Hodgson reported that the mixing angle is related to the parameter,  $F_p/4H$ , where  $H$  is the height of louver. A schematic drawing of the test results by Pauley and Hodgson is illustrated in Fig. 8. As seen in this figure, for  $F_p/4H = 1, 1.5$ , and 2, the mixing angles increase with the Reynolds number. However, for  $F_p/4H = 3$ , the mixing angle decreases with an increase of the Reynolds number. Based on their flow visualization experiments, Pauley and Hodgson argued that an inviscid Rayleigh instability may cause the unsteadiness of the shear layer for  $F_p/4H = 3$ . The velocity difference across the shear layer was large enough to cause vortex rollup, and the mixing region was contained primarily within the louvers and did not extend between the fin rows. Therefore a decrease of mixing angle and lower heat transfer performance is shown. Examination of the present  $F_p/4H$  values are approximately 1.14 ( $F_p = 1.21$  mm), 1.6 ( $F_p = 1.69$  mm), and 2.4 ( $F_p = 2.54$  mm). Therefore, for  $F_p = 2.54$  mm it is very likely that the mixing angle may not increase with the Reynolds number compared to  $F_p = 1.69$  and 1.21. Consequently, a significant degradation of heat transfer performance was seen for a convex-louver fin having  $F_p = 2.54$  mm. Similar results were also seen for the 4-row configuration.

Figure 9 illustrates the effect of the tube row number on the heat transfer and friction characteristics for a given fin pitch ( $F_p = 2.54$  mm). The experimental data indicate that the fric-

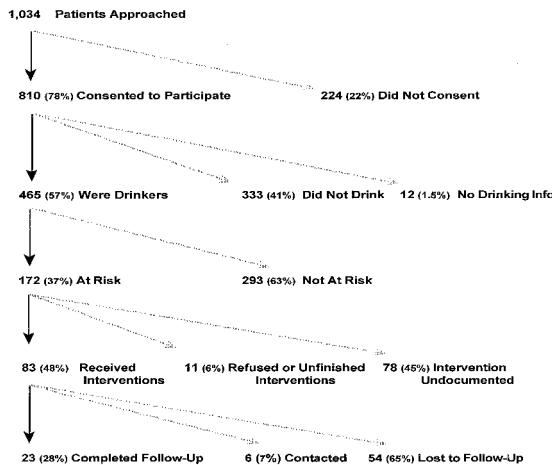


Fig. 6 Percent reduction for convex-louver fin surface by using the VG-1 criteria.

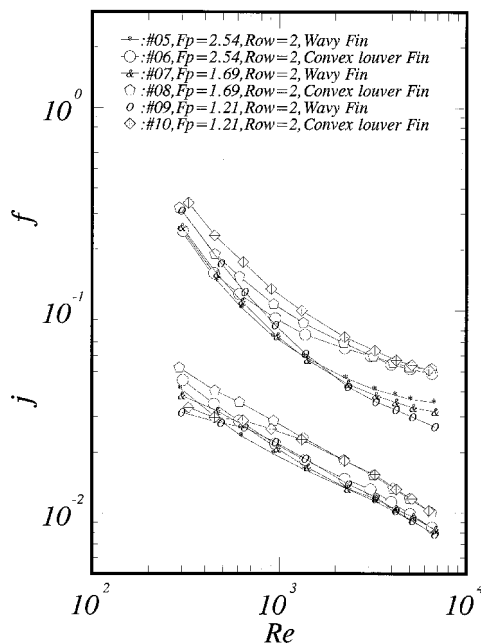


Fig. 7 Effect of fin pitch on the heat transfer and friction characteristics.

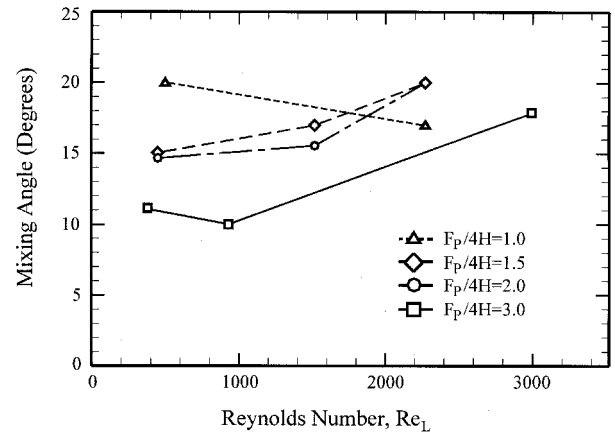


Fig. 8 Mixing angle vs  $Re_L$  for  $\theta = 19$  deg. Quoted from the test results by Pauley and Hodgson.<sup>22</sup>

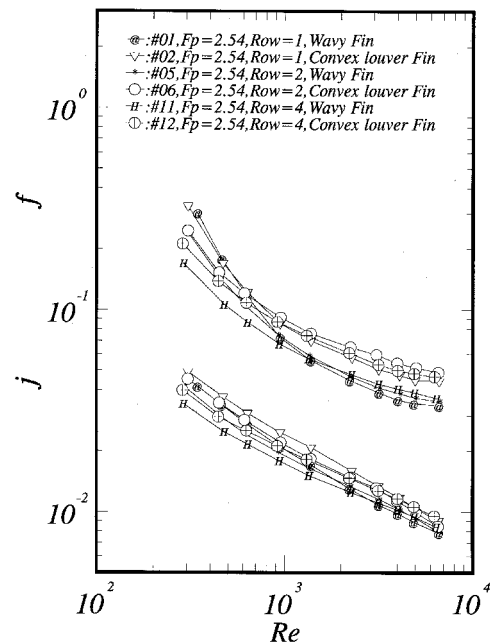


Fig. 9 Effect of tube row on heat transfer and friction characteristics ( $F_p = 2.54$  mm).

tion factors are not affected by the row number for both wavy and convex-louver configurations. It is interesting to see that the friction factors for the 1-row coil are nearly the same as those of multirow coils. The effects of the number of tube rows on the heat transfer performance are more pronounced than those of friction factors. For  $Re_{D_c} < 2 \times 10^3$ , an approximately 15% lower heat transfer performance is seen for the 4-row coil as compared to the 1-row coil. The effect diminishes for  $Re_{D_c} > 2.5 \times 10^3$ . Similar results are also seen for the wavy fin geometry. The effect of the number of tube rows for  $F_p = 1.21$  mm, however, shows different characteristics, as given in Fig. 10. A significant reduction of heat transfer performances are displayed for both wavy and convex-louver fin configurations. Compared to a wavy fin configuration, the reduction for 4-row coils exceeds the 1-row coil by more than 100% at  $Re_{D_c} = 8 \times 10^2$ . The pronounced reduction for a wavy fin configuration with an increase in the number of the tube row for  $F_p = 1.21$  mm may be explained from the flow visualization experiments conducted by Ali and Ramadhyani.<sup>23</sup> Ali and Ramadhyani showed that the thermal-hydraulic characteristics of corrugated channels were strongly related to the ratio  $b/L_c$ , where  $L_c$  is the wavelength of the corrugated channel. For  $b/L_c = 0.23$ , Ali and Ramadhyani observed the presence of both spanwise and longitudinal eddies formed beginning at the fourth facet, and this caused good mixing downstream. However, as  $b/L_c$  reduced to 0.15, only longitudinal eddies were observed, and, consequently, the degree of mixing was reduced. Note that the values of  $b/L_c$  are 0.115 and 0.255 for  $F_p = 1.21$  and 2.54 mm, respectively. The degradation is even more pronounced for the convex-louver fin configuration, as reported by the flow visualization of convex-louver fin experiments conducted by Pauley and Hodgson.<sup>22</sup> Their experiments show that a recirculation region often appeared in the sheltered area formed by the apex angle of the chevron, and the trapped fluid under the sheltered area often cannot be ejected into the mainstream at low Reynolds numbers. The recirculation region is likely to enlarge as fluid approaches from upstream. The numerical simulation results by previous investigators<sup>24,25</sup> also indicated this phenomenon. As a result, lower heat transfer coefficients are encountered as the row number increases. However, as the Reynolds number increases, the mixing angle increases and the ejected rate of the trapped liquid under the sheltered area increases significantly. This eventually results in a negligible effect of the number of tube rows in this range.

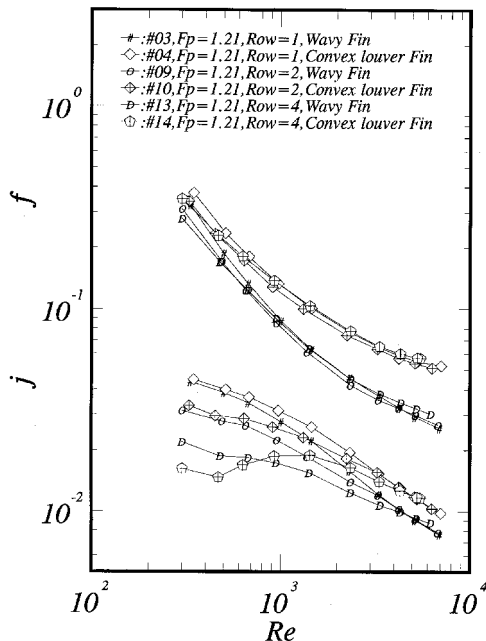


Fig. 10 Effect of tube row on heat transfer and friction characteristics ( $F_p = 1.21$  mm).

### Correlation Results of $j$ for Convex-Louver Fin Geometry

It is obvious from the curves shown in Figs. 7, 9, and 10 that no single curve can be expected to describe the complex behavior of the convex-louver fin for both  $j$  and  $f$  factors. As a result, a multiregression is carried out to obtain the appropriate correlation form of  $j$  and  $f$  for the convex-louver configuration. The database includes previous work<sup>8</sup> and the present test results. It is recommended that the following equations are used to describe the  $j$  and  $f$ :

$$j = 16.06 Re_{D_c}^{-1.02(P_f/D_c)^{-0.256}} (A_o/A_i)^{-0.601} N^{-0.069} (P_f/D_c)^{0.84} \quad (18)$$

The recommended correlation for friction factors when  $Re_{D_c} < 1 \times 10^3$  is

$$f = 0.264[0.105 + 0.708 \exp(-Re_{D_c}/225)] Re_{D_c}^{-0.637} \times (A_o/A_i)^{0.263} (P_f/D_c)^{-0.317} \quad (19)$$

For  $Re_{D_c} > 1 \times 10^3$

$$f = 0.768[0.0494 + 0.142 \exp(-Re_{D_c}/1180)] (A_o/A_i)^{0.0195} \times (P_f/D_c)^{-0.121} \quad (20)$$

As shown in Fig. 11, Eq. (18) can describe 82.2% of the experimental data within 10%, Eq. (19) can describe 90.7% of the experimental data within 15%, and Eq. (20) can describe 95.9% of the experimental data within 15%. Note that the  $j$  factor correlation overpredicts the test results of the 4-row configuration and  $F_p = 1.21$  mm. However, in practical applications, the convex-louver fin-and-tube heat exchangers are employed with a 1- or 2-row configuration.

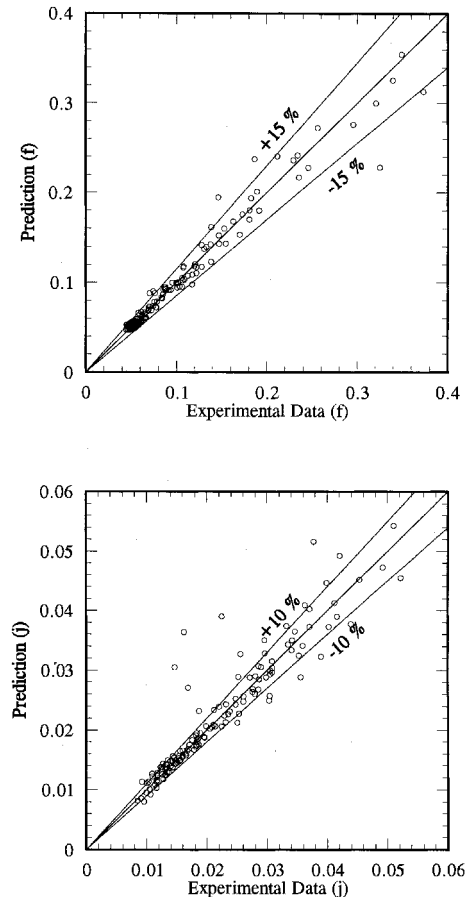


Fig. 11 Comparison of  $j$  and  $f$  using the present correlations.

## Conclusions

Heat transfer and friction characteristics of plate fin-and-tube heat exchangers having convex-louver and wavy configurations are carried out in the present study. A total of 14 samples were tested. Based on the aforementioned discussions, the following conclusions are drawn:

- 1) The number of tube rows does not affect the friction factor for both wavy and convex-louver fin geometry.
- 2) For the wavy fin having a multiple-row configuration the effect of fin pitch on heat transfer performance is negligible. Converse to the results of wavy fin configuration the convex-louver fin exhibits a dependence of fin pitch. For a 1-row configuration, both convex-louver and wavy fin show that the heat transfer coefficients increase with a decrease of fin pitch.
- 3) The effect of the number of tube rows on heat transfer performance changes significantly with the fin pitch. For  $F_p = 2.54$  mm, the effect is very small. However, significant differences are seen as  $F_p$  decreases to 1.21 mm. The differences are especially pronounced for  $Re_{De} < 2 \times 10^3$ . For  $Re_{De} > 2 \times 10^3$ , the effect of the tube row number diminishes as a result of vortex shedding caused by the tube row.

## Acknowledgments

The authors express their gratitude for the Energy R&D foundation funding from the Energy Commission of the Ministry of Economic Affairs, Taiwan, for providing the financial support of this study. The suggestions by Ralph Webb for improving the contents of the manuscript are very much appreciated.

## References

- <sup>1</sup>Giovannoni, F., and Mattarolo, L., "Experimental Researches on the Finned Tube Heat Exchangers with Corrugated Fins," *Proceedings of the 16th International Congress of Refrigeration* (Paris, France), No. B.1-493, 1983, pp. 215–220.
- <sup>2</sup>Beecher, D. T., and Fagan, T. J., "Effects of Fin Pattern on the Air-Side Heat Transfer Coefficient in Plate Finned-Tube Heat Exchangers," *American Society of Heating, Refrigeration and Air-Conditioning Engineers Transactions*, Vol. 93, No. 2, 1987, pp. 1961–1984.
- <sup>3</sup>Wang, C.-C., Fu, W. L., and Chang, C. T., "Heat Transfer and Friction Characteristics of Typical Wavy Fin-and-Tube Heat Exchangers," *Experimental Thermal and Fluid Science*, Vol. 14, No. 2, 1997, pp. 174–186.
- <sup>4</sup>Chang, W. R., Wang, C.-C., Tsai, W. C., and Shyu, R. J., "Air Side Performance of Louver Fin Heat Exchanger," *Proceedings of the 4th ASME/JSME Thermal Engineering Joint Conference*, Vol. 4, The American Society of Mechanical Engineers, New York, 1995, pp. 367–372.
- <sup>5</sup>Wang, C.-C., Chang, Y. P., Chi, K. Y., and Chang, Y. J., "A Study of Non-Redirection Louver Fin-and-Tube Heat Exchangers," *Proceedings of the Institute of Mechanical Engineering, Part C, Journal of Mechanical Engineering Science* (to be published).
- <sup>6</sup>Wang, C.-C., Chang, Y. P., Chi, K. Y., and Chang, Y. J., "An Experimental Study of Heat Transfer and Friction Characteristics of Typical Louver Fin and Tube Heat Exchangers," *International Journal of Heat and Mass Transfer*, Vol. 41, No. 4–5, 1998, pp. 817–822.
- <sup>7</sup>Hatada, T., Ueda, U., Oouchi, T., and Shimizu, T., "Improved Heat Transfer Performance of Air Coolers by Strip Fins Controlling Air Flow Distribution," *ASHRAE Transactions*, Vol. 95, No. 2, 1989, pp. 166–170.
- <sup>8</sup>Wang, C.-C., Chen, P. Y., and Jang, J. Y., "Heat Transfer and Friction Characteristics of Convex-Louver Fin-and-Tube Heat Exchangers," *Experimental Heat Transfer*, Vol. 9, No. 1, 1996, pp. 61–78.
- <sup>9</sup>*ASHRAE Handbook Fundamental*, SI-Edition, American Society of Heating, Refrigerating and Air-Conditioning Engineers, Inc., Atlanta, GA, 1993, pp. 14, 15, Chap. 13.
- <sup>10</sup>*Standard Methods for Laboratory Air-Flow Measurement*, American Society of Heating, Refrigerating and Air-Conditioning Engineers, Standard 41.2-1987, Atlanta, GA, 1987.
- <sup>11</sup>McQuiston, F. C., and Parker, J. D., *Heating, Ventilating, and Air-Conditioning*, 4th ed., Wiley, New York, 1994, p. 571, Chap. 14.
- <sup>12</sup>Gnielinski, V., "New Equation for Heat and Mass Transfer in Turbulent Pipe and Channel Flow," *International Chemical Engineering*, Vol. 16, 1976, pp. 359–368.
- <sup>13</sup>Schmidt, T. E., "Heat Transfer Calculations for Extended Surfaces," *Refrigerating Engineering*, April, 1949, pp. 351–357.
- <sup>14</sup>Kays, W. M., and London, A. L., *Compact Heat Exchangers*, 3rd ed., McGraw-Hill, New York, 1984.
- <sup>15</sup>Moffat, R. J., "Describing the Uncertainties in Experimental Results," *Experimental Thermal and Fluid Science*, Vol. 1, No. 1, 1988, pp. 3–17.
- <sup>16</sup>O'Brien, J. E., and Sparrow, E. M., "Corrugated-Duct Heat Transfer, Pressure Drop, and Flow Visualization," *Journal of Heat Transfer*, Vol. 104, No. 3, 1982, pp. 410–416.
- <sup>17</sup>Sparrow, E. M., and Comb, J. W., "Effect of Interwall Spacing and Fluid Flow Inlet Conditions on a Corrugated-Wall Heat Exchangers," *International Journal of Heat and Mass Transfer*, Vol. 26, No. 7, 1983, pp. 993–1005.
- <sup>18</sup>Molki, M., and Yuen, C. M., "Effect of Interwall Spacing on Heat Transfer and Pressure Drop in a Corrugated-Wall Duct," *International Journal of Heat and Mass Transfer*, Vol. 29, No. 7, 1986, pp. 987–997.
- <sup>19</sup>Webb, R. L., *Principles of Enhanced Heat Transfer*, Wiley, New York, 1994, Chap. 3.
- <sup>20</sup>Rich, D. G., "The Effect of Fin Spacing on the Heat Transfer and Friction Performance of Multi-Row, Plate Fin-and-Tube Heat Exchangers," *ASHRAE Transactions*, Vol. 79, No. 2, 1973, pp. 137–145.
- <sup>21</sup>Wang, C.-C., Chang, Y. J., Hsieh, Y. J., and Lin, Y. T., "Sensible Heat Transfer Characteristics of Plate Fin-and-Tube Heat Exchangers Having Plane Fins," *International Journal of Refrigeration*, Vol. 19, No. 4, 1996, pp. 223–230.
- <sup>22</sup>Pauley, L. L., and Hodgson, J. E., "Flow Visualization of Convex Louver Fin Arrays to Determine Maximum Heat Transfer Conditions," *Experimental Thermal and Fluid Science*, Vol. 9, No. 1, 1994, pp. 53–60.
- <sup>23</sup>Ali, M. M., and Ramadhyani, S., "Experiments on Convective Heat Transfer in Corrugated Channels," *Experimental Heat Transfer*, Vol. 5, 1992, pp. 175–193.
- <sup>24</sup>Bemisderfer, C. H., "Heat Transfer: A Contemporary Analytical Tool for Developing Improved Heat Transfer Surfaces," *ASHRAE Transactions*, No. 1, 1987, pp. 1157–1167.
- <sup>25</sup>Matsushima, H., Hatada, T., Endo, T., and Senshu, T., "Three-Dimensional Simulation of Forced Convection and Heat Transfer in Heat Exchangers with Convex Strip Fins by the Finite Element Method," American Society of Mechanical Engineers, Paper 91-HT-18, New York, 1991.